The Journal of International Medical Research
2010; 38: 686 – 693

A Unique Magnetic Resonance Imaging Feature of Glioblastoma Multiforme: the 'Pseudopalisade' Sign

BC Huang, DY Geng, CS Zee, YM Ji, HX Cheng and YM Dai

Department of Radiology, Huashan Hospital, Fudan University, Shanghai, China

This study was designed to investigate the unique magnetic resonance imaging (MRI) appearance of histopathologically-proven glioblastoma multiforme (GBM) with pseudopalisade necrosis and to assess its value for grading gliomas and providing a differential diagnosis. The study included 169 patients with intracranial masses who underwent surgery and had a proven histopathological diagnosis: 50 with GBM, 77 with gliomas (46 grade II and 31 grade III) and 42 with other intracranial masses (20 metastases, 14 lymphomas and eight abscesses). All patients underwent pre-operative brain MRI including post-contrast T_1-weighted imaging. The presence of the 'pseudopalisade' sign on post-contrast T_1-weighted images was compared among the different types of brain mass. The frequency of the 'pseudopalisade' sign in GBMs (94.00%) was significantly higher than that seen in grade II and III gliomas (11.69%) and other intracranial masses (7.14%). The 'pseudopalisade' sign on post-contrast T_1-weighted images was useful for grading gliomas and for differentiating GBM from other brain masses.

KEY WORDS: Glioblastoma multiforme (GBM); Glioma; Magnetic resonance imaging; Pseudopalisading; Pseudopalisade sign

Introduction

Glioblastoma multiforme (GBM) is the most common and most malignant astrocytoma.[1] The mortality and disability rates associated with GBM are among the highest for astrocytomas,[2] so early diagnosis and surgical treatment with adjunct radiation and chemotherapy are key to prolonging a patient's life and to improving their quality of life. Currently, the diagnosis of GBM is largely dependent on magnetic resonance imaging (MRI). GBMs typically have irregular contrast enhancement, which is often ring-like.[3] The mass lesion is surrounded by significant oedema, with a resultant mass effect that can be severe enough to cause herniation.[3] The conventional radiological characteristics of brain metastatic disease include a peripheral location, spherical shape, ring enhancement and multiple lesions.[4] Malignant astrocytomas and metastases usually have no typical features on routine MRI to differentiate one from the other.

Recently, advanced MRI techniques, such as diffusion-weighted imaging, MR spectroscopy and perfusion-weighted imaging, have provided additional

information for the differential diagnosis of various brain tumours. In order to distinguish glioblastoma from metastatic disease, most of the new MRI techniques rely on detecting differences in the peri-tumoural region. In metastatic disease, for example, this area consists of vasogenic oedema, whereas in glioma, neoplastic cells may also be present.[5,6] Several groups have shown that perfusion-weighted imaging and MR spectroscopy of the peri-tumoural region can be used to differentiate between a solitary metastasis and a high-grade glioma.[7,8] Diffusion tensor imaging has also shown promise in this area.[9,10] Although advances in MRI techniques have shown some promising results in grading of gliomas and differentiating GBMs from metastatic disease,[9,11,12] these techniques require extra sequence time, and sophisticated MRI hardware and software, post-processing and additional interpretation skills and time.

In most institutions, the diagnosis of GBMs is still largely dependent on routine MRI findings. It was, therefore, of interest to try and identify any special characteristics of GBM using routine MRI that may provide additional information that would be useful for making a correct and timely diagnosis. The pseudopalisading features of GBM, with attenuated clusters of nuclei surrounding areas of necrosis in a characteristic garland-like arrangement of rows, were initially reported by neuropathologists.[13] Notably, pseudopalisades were shown to be associated with necrosis and were nearly always present as a pathological feature of GBM.[14] In fact, pseudopalisading necrosis has been incorporated into the pathological definition of glioblastoma, distinguishing it from lower grade astrocytomas.[13,14] Because pseudopalisading necrosis is a pathological hallmark that distinguishes GBM from lower grade astrocytomas, this study was designed to investigate whether the histopathological features of pseudopalisading necrosis could also be seen on routine MRI.

Patients and methods

CLINICAL DATA

In this observational study, patients with intracranial masses who were operated upon at the Huashan Hospital, Fudan University, Shanghai, China, were enrolled sequentially between 2003 and 2008. Eligibility was based on medical records and a picture archiving and communication system. All patients had routine MRI scans of the brain including post-contrast T_1-weighted images before surgical resection.

After studying the post-contrast T_1-weighted images of all GBMs, the unique MRI feature of GBM was named as the 'pseudopalisade' sign. The criteria for the 'pseudopalisade' sign on post-contrast T_1-weighted images included: (i) many elliptical bubbles of the same or similar size; (ii) complete bubbles with a soft bubble margin that resembled mastoid cells; and (iii) enhancement of the bubble's margin with an absence of enhancement in the centre of the bubble. The MRI images of all patients were interpreted by three senior neuroradiologists according to the same criteria and consensus reached.

Informed consent was obtained from all patients for routine MRI studies and for review of the patients' records and images. The study was performed with the approval of the Institutional Review Board of Huashan Hospital, Fudan University, Shanghai, China.

HISTOLOGICAL TECHNIQUES

All tissues were fixed separately in 10% formalin solution for < 24 h, and prepared by routine paraffin embedding and the cutting of sequential 5 µm sections.

Haematoxylin and eosin stain was used according standard protocols to visualize tissue sections.

MRI SEQUENCE AND PARAMETERS

Imaging was performed with a 1.5-T MRI unit (Signa Excite HD 1.5T™ Twinspeed; GE Healthcare Biosciences, Piscataway, NJ, USA) or a 3.0-T MRI unit (Signa Excite GEMSOC01; GE Healthcare Biosciences). Localizing sagittal T_1-weighted images were obtained, followed by transverse T_1-weighted (2214/18.3 [repetition time in ms/echo time in ms]), 6 mm slice thickness, 2 mm interslice gap, 24 cm field of view, and 320 × 224 matrix, post-contrast transverse (2214/18.3) and sagittal T_1-weighted images. Contrast agent (gadolinium diethylenetriamine penta-acetic acid) was injected at a rate of 1 ml/s and at a dose of 0.1 mmol/kg.

CT SCANNING

Routine computed tomography (CT) scanning of the mastoid cells in the bone window of the head was carried out using a Siemens Somatom Emotion 6 CT scanner (Siemens AG, Erlangen, Germany). Routine head CT scanning was performed for 12 slices each 10 mm thick.

STATISTICAL ANALYSIS

All statistical analyses were carried out using the SPSS® statistical package, version 13.0 (SPSS Inc., Chicago, IL, USA) for Windows®. The χ^2-test was used to analyse the frequency of the 'pseudopalisade' sign in the MRI scans of GBM, grade II and III gliomas, and other intra-cranial masses. A P-value < 0.05 was considered to be statistically significant.

Results

The study included 169 patients with intracranial masses: 50 GBMs, 77 gliomas (46 grade II and 31 grade III) and 42 other intracranial masses (20 metastases, 14 lymphomas and eight abscesses). Of the 50 patients with GBMs, there were 16 women and 34 men with a mean age of 51 years (range 4 – 75 years). The locations of the GBMs were as follows: four in the parietal lobe, 17 in the frontal lobe, 17 in the temporal lobe, four in the triangular areas, three in the cerebellum and five in other areas. Of the 77 patients with gliomas, there were 28 women and 49 men with a mean age of 40 years (range 7 – 76 years). Of the 42 other intracranial masses, there were 17 women and 25 men with a mean age of 52 years (range 26 – 72 years).

Analysis of post-contrast T_1-weighted images of all GBMs allowed definition of the characteristics of the 'pseudopalisade' sign, which consisted of many same or similar sized elliptical bubbles resembling mastoid cells. Enhancement of the margin, but not the centre, of the bubbles was observed. The 'pseudopalisade' sign corresponded to the pseudopalisading necrosis observed in histopathological specimens (Fig. 1) and was seen in almost all GBMs (Fig. 2). Table 1 shows the frequency of the 'pseudopalisade' sign in the various types of intracranial mass and this was analysed by the χ^2-test. There was a statistically significant difference between the frequency of the 'pseudopalisade' sign in GBMs compared with grade II and III gliomas ($P < 0.05$), and between GBMs and other intracranial masses ($P < 0.05$). The 'pseudopalisade' sign was not observed in only three of the 50 GBMs, because of intratumoural haemorrhage. It was seen in a few cases of grade III gliomas (19.35%), but only infrequently in grade II gliomas (6.52%) and other intracranial masses (7.14%) such as metastases and lymphoma, and not in any of the abscesses. The majority of grade II and III gliomas (Fig. 3) and other intracranial

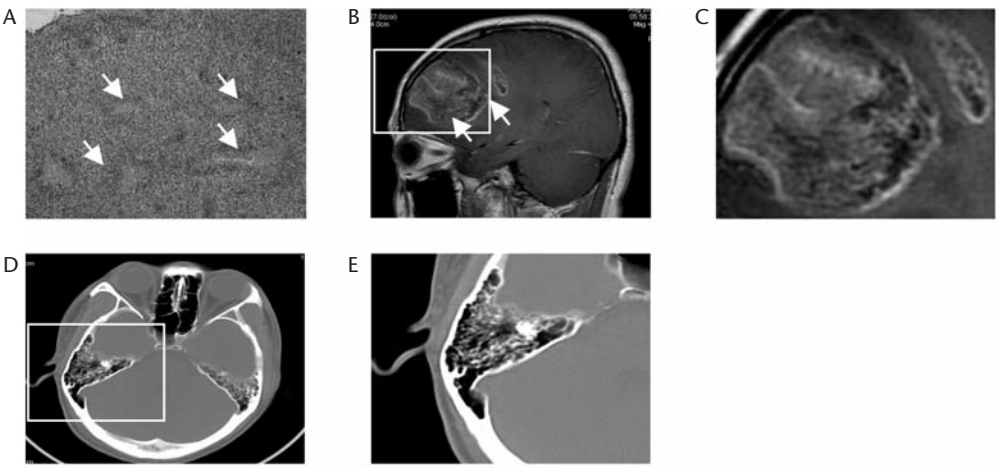

FIGURE 1: Images from a 27-year old man with a right frontal glioblastoma multiforme (GBM). (A) Light photomicrograph showing the features of pseudopalisading necrosis (white arrows) with attenuated clusters of nuclei surrounding many areas of necrosis in a characteristic garland-like arrangement of rows (haematoxylin and eosin, × 400 original magnification). (B) Pre-operative sagittal post-contrast T_1-weighted image showing the typical 'pseudopalisade' sign (white arrows). (C) Higher magnification of the area shown in B. (D) Computed tomography scan showing whole and soft elliptical bubbles that resemble the 'pseudopalisade' sign. (E) Higher magnification of the area shown in D

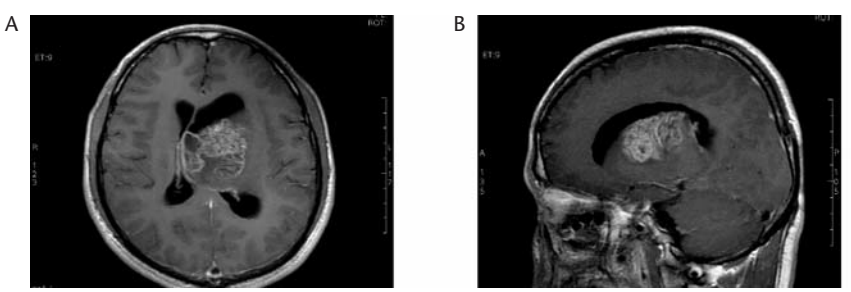

FIGURE 2: Post-contrast T_1-weighted magnetic resonance images from a 37-year old man with a left thalamus glioblastoma multiforme clearly showing the 'pseudopalisade' sign: (A) transverse plane; and (B) sagittal plane

masses (Fig. 4) did not, however, show evidence of the 'pseudopalisade' sign.

Discussion

One pathological feature that distinguishes GBMs from lower grade astrocytomas that may explain the abrupt change in biological behaviour is pseudopalisading necrosis, a dense collection of neoplastic cells that surround a central necrotic focus.[14] The origins and potential function of pseudopalisades in tumourigenesis have remained obscure since their recognition in the early 1900s.[13] The first indication of their central role in glioblastoma biology was the discovery that they express high levels of

TABLE 1:
Frequency of the 'pseudopalisade' sign on magnetic resonance images of the brain from 169 patients with different intracranial masses

	Glioblastoma multiforme (*n* = 50)	Grade II and III gliomas (*n* = 77)	Other intracranial masses (*n* = 42)
'Pseudopalisade' sign present (*n*)	47	9 Grade II: 3/46 Grade III: 6/31	3 Metastases: 2/20 Lymphomas: 1/14 Abscesses: 0/8
Frequency	94.00%	11.69%	7.14%
P-value[a]		< 0.05	< 0.05

[a]Compared with the frequency in glioblastoma multiforme samples (χ^2-test).

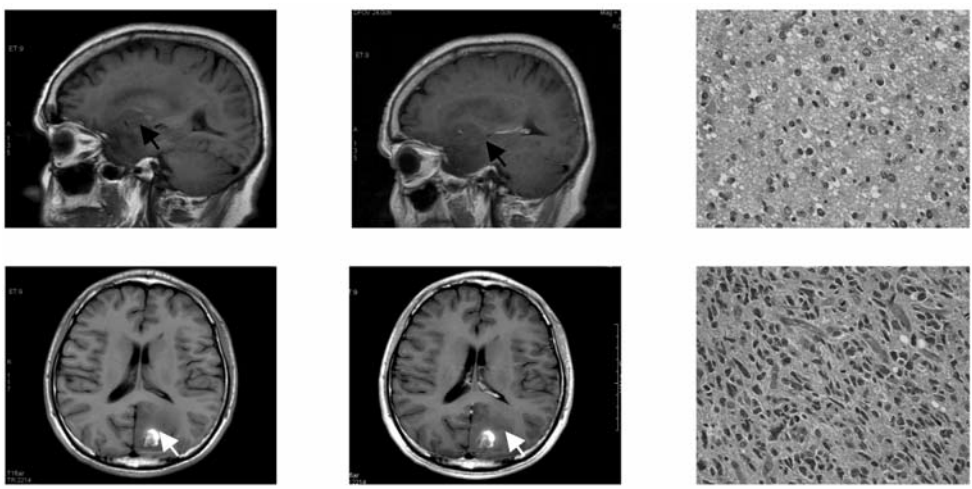

FIGURE 3: The 'pseudopalisade' sign was not generally seen in grade II and III gliomas. The left hand images are pre-contrast T_1-weighted magnetic resonance images (MRIs), the centre images are post-contrast T_1-weighted MRIs, and the right hand images are light photomicrographs (haematoxylin and eosin, × 400 original magnification). The top row of images are from a 68-year old woman with a right grade II astrocytoma (black arrows) without evidence of the 'pseudopalisade' sign. The bottom row of images are from a 17-year old man with a left occipital grade III astrocytoma (white arrows) without evidence of the 'pseudopalisade' sign

hypoxia-inducible regulators of angiogenesis, including vascular endothelial growth factor and interleukin-8, which promote new vasculature and drive rapid tumour growth.[15,16] More recent studies have shown that angiogenesis may initiate pseudopalisade formation, hypoxia and necrosis in glioblastomas.[17] Some studies have proposed that pseudopalisades represent a wave of tumour cells actively migrating away from a central hypoxic zone that is created following vascular compromise and that is associated with intravascular thrombosis.[18] Hypoxic up-regulation of tissue

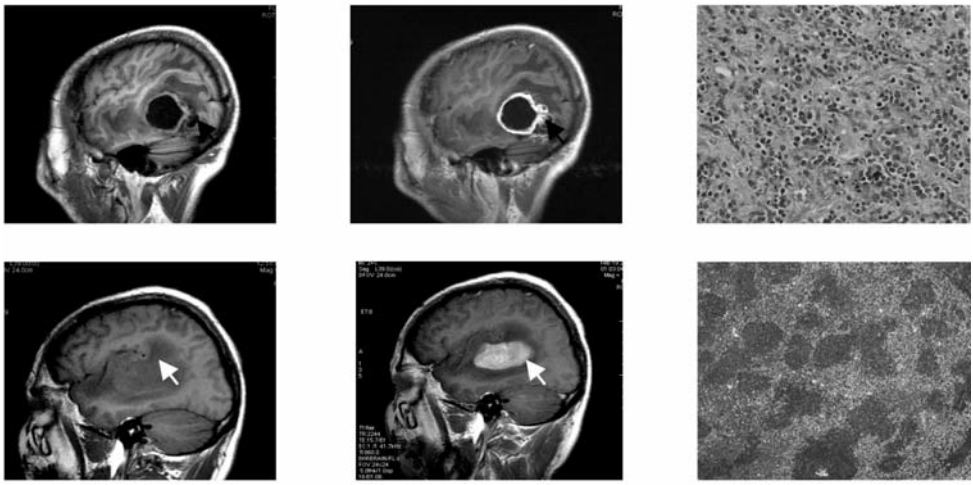

FIGURE 4: The 'pseudopalisade' sign was not generally seen in other intracranial masses. The left hand images are pre-contrast T_1-weighted magnetic resonance images (MRIs), the centre images are post-contrast T_1-weighted MRIs, and the right hand images are light photomicrographs (haematoxylin and eosin, × 400 original magnification). The top row of images are from a 47-year old woman with a left temple metastatic adenocarcinoma (black arrows) without evidence of the 'pseudopalisade' sign. The bottom row of images are from a 56-year old man with a left frontal B cell lymphoma (white arrows) without evidence of the 'pseudopalisade' sign

factor by gliomas would then follow the initial angiopoietin-2-mediated vascular insult and accentuate tumour hypoxia due to intravascular thrombosis.[19 – 21]

The present study has confirmed that the pseudopalisading observed in routine histopathological examinations of GBMs can be clearly detected on post-contrast T_1-weighted MRIs and that it is a special feature of GBMs. In pathology, the features of pseudopalisading necrosis have been incorporated into the pathological definition of glioblastoma.[14] As the MRI features corresponded to the histopathological features of pseudopalisading necrosis, we have called it the 'pseudopalisade' sign. It consisted of many of the same or similar sized, whole and soft elliptical bubbles that resembled mastoid cells. There was enhancement of the margin of the bubbles, but not at the centre. The bubbles that formed the 'pseudopalisade' sign were due to micronecrosis or microcysts.

In the present study, the 'pseudopalisade' sign was seen in almost all GBMs, with only three tumours showing no 'pseudopalisade' signs because of intratumoural haemorrhage. The 'pseudopalisade' sign was seen in a few cases of grade III gliomas (19.35%), but only infrequently in grade II gliomas (6.52%) and other intracranial masses (7.14%). We suggest that, as for the pseudopalisading necrosis that is associated with GBMs in histopathology, the 'pseudopalisade' sign seen on MRI may help to discriminate GBMs from grade II and III gliomas and other intracranial masses such as metastases, lymphomas and abscesses.

The different histopathological appearance of GBM, grade II and III gliomas, and other

intracranial masses such as metastases, lymphomas and abscesses may explain why the 'pseudopalisade' sign is the hallmark of GBMs on MRI rather than of grade II and III gliomas and other intracranial masses. Pseudopalisading features are formed by attenuated clusters of nuclei surrounding the areas of necrosis in a characteristic garland-like arrangement of rows. Notably, pseudopalisades are associated with necrosis and are nearly always pathological features of glioblastomas. Cells in necrotic areas unable to survive the decreased oxygen tensions succumb and form the nidus of coagulation necrosis. Other cells, however, begin migrating to the periphery of the hypoxic field in moving waves (pseudopalisades).[14] Areas of necrosis with their margins formed by migrating pseudopalisading cells constitute the 'pseudopalisade' sign of GBM on post-contrast T_1-weighted images. Since there is no micronecrosis in grade II gliomas and only occasional slight micronecrosis in grade III gliomas, the 'pseudopalisade' sign was rarely found in grade II gliomas, and only occasionally found in grade III gliomas. Necrosis could happen in other intracranial masses such as metastases, lymphomas and abscesses, but the shape and size of the necrotic areas are usually irregular, with ring enhancement seen on post-contrast T_1-weighted MRIs.[22]

Advanced MRI techniques have not become widely available because of the requirement for extra imaging time, sophisticated MRI hardware and software, post-processing and additional interpretation skills and time. Thus, the diagnosis of GBM is still primarily dependent upon routine MRI. Identification of the 'pseudopalisade' sign on post-contrast T_1-weighted MRIs could help diagnose GBM in the absence of advanced MRI techniques. Of course, if available, more advanced MRI techniques might provide additional information to enhance the diagnostic capability of routine MRI.

There are some limitations to the present study. It was not possible to undertake a correlative study to investigate any associations between the 'pseudopalisade' sign and the mass size, the tumour position and the proliferation index of the tumour. A comparative study should be performed to investigate the clinical utility of using the 'pseudopalisade' sign on routine MRI compared with more advanced MRI techniques. Nevertheless, this study has shown that the 'pseudopalisade' sign is a common feature of GBMs on post-contrast T_1-weighted MRIs, and it can be used to grade gliomas and to differentiate GBMs from other brain masses before surgery.

Acknowledgement

This work was supported by research grants to Dr Dao Ying Geng from the National Great Research Project (2007CB935803).

Conflicts of interest

The authors had no conflicts of interest to declare in relation to this article.

• Received for publication 13 September 2009 • Accepted subject to revision 23 October 2009
• Revised accepted 22 January 2010

References

1 Falini A, Calabrese G, Origgi D, *et al*: Proton magnetic spectroscopy and intracranial tumors: clinical perspectives. *J Neurol* 1996; **243:** 706 – 714.

2 Louis DN, Holland EC, Cairncross JG: Glioma classification: a molecular reappraisal. *Am J Pathol* 2001; **159:** 779 – 786.

3 DeAngelis LM: Brain tumors. *N Engl J Med* 2001; **344:** 114 – 123.
4 Stuckey SL, Wijedeera R: Multicentric/multifocal cerebral lesions: can fluid-attenuated inversion recovery aid the differentiation between glioma and metastases? *J Med Imaging Radiat Oncol* 2008; **52:** 134 – 139.
5 Kelly PJ, Daumas-Duport C, Scheithauer BW, *et al*: Stereotactic histologic correlations of computed tomography and magnetic resonance imaging-defined abnormalities in patients with glial neoplasms. *Mayo Clin Proc* 1987; **62:** 450 – 459.
6 Zhang M, Olsson Y: Hematogenous metastases of the human brain – characteristics of peritumoral brain changes: a review. *J Neurooncol* 1997; **35:** 81 – 89.
7 Chiang IC, Kuo YT, Lu CY, *et al*: Distinction between high-grade gliomas and solitary metastases using peritumoral 3-T magnetic resonance spectroscopy, diffusion, and perfusion imagings. *Neuroradiology* 2004; **46:** 619 – 627.
8 Law M, Cha S, Knopp EA, *et al*: High grade gliomas and solitary metastases: differentiation by using perfusion and proton spectroscopic MR imaging. *Radiology* 2002; **222:** 715 – 721.
9 Tsuchiya K, Fujikawa A, Nakajima M, *et al*: Differentiation between solitary brain metastasis and high-grade glioma by diffusion tensor imaging. *Br J Radiol* 2005; **78:** 533 – 537.
10 Lu S, Ahn D, Johnson G, *et al*: Peritumoral diffusion tensor imaging of high-grade gliomas and metastatic brain tumors. *AJNR Am J Neuroradiol* 2003; **24:** 937 – 941.
11 Tien RD, Felsberg GJ, Friedman H, *et al*: MR imaging of high-grade cerebral gliomas: value of diffusion-weighted echoplanar pulse sequences. *AJR Am J Roentgenol* 1994; **162:** 671 – 677.
12 Tang YM, Ngai S, Stuckey S: The solitary enhancing cerebral lesion: can FLAIR aid the differentiation between glioma and metastasis? *AJNR Am J Neuroradiol* 2006; **27:** 609 – 611.
13 Rong Y, Post DE, Pieper RO, *et al*: PTEN and hypoxia regulate tissue factor expression and plasma coagulation by glioblastoma. *Cancer Res* 2005; **65:** 1406 – 1413.
14 Wippold FJ, Lämmle M, Anatelli F, *et al*: Neuropathology for the neuroradiologist: palisades and pseudopalisades. *AJNR Am J Neuroradiol* 2006; **27:** 2037 – 2041.
15 Plate KH, Breier G, Weich HA, *et al*: Vascular endothelial growth factor is a potential tumour angiogenesis factor in human gliomas *in vivo*. *Nature* 1992; **359:** 845 – 848.
16 Desbaillets I, Diserens AC, Tribolet N, *et al*: Upregulation of interleukin 8 by oxygen-deprived cells in glioblastoma suggests a role in leukocyte activation, chemotaxis, and angiogenesis. *J Exp Med* 1997; **186:** 1201 – 1212.
17 Zagzag D, Lukyanov Y, Lan L, *et al*: Hypoxia-inducible factor 1 and VEGF upregulate CXCR4 in glioblastoma: implications for angiogenesis and glioma cell invasion. *Lab Invest* 2006; **86:** 1221 – 1232.
18 Brat DJ, Castellano-Sanchez AA, Hunter SB, *et al*: Pseudopalisades in glioblastoma are hypoxic, express extracellular matrix proteases, and are formed by an actively migrating cell population. *Cancer Res* 2004; **64:** 920 – 927.
19 Hamada K, Kuratsu J, Saitoh Y, *et al*: Expression of tissue factor correlates with grade of malignancy in human glioma. *Cancer* 1996; **77:** 1877 – 1883.
20 Contrino J, Hair G, Kreutzer DL, *et al*: *In situ* detection of tissue factor in vascular endothelial cells: correlation with the malignant phenotype of human breast disease. *Nat Med* 1996; **2:** 209 – 215.
21 Amirkhosravi A, Meyer T, Warnes G, *et al*: Pentoxifylline inhibits hypoxia-induced upregulation of tumor cell tissue factor and vascular endothelial growth factor. *Thromb Haemost* 1998; **80:** 598 – 602.
22 Soffietti R, Ruda R, Mutani R: Management of brain metastases. *J Neurol* 2002; **249:** 1357 – 1369.

Author's address for correspondence
Dr Bing Cang Huang
Department of Radiology, Huashan Hospital, Fudan University, Wu Lu Mu Qi Zhong Road, Shanghai 200040, China.
E-mail: hbc9209@163.com